Chemical and mechanical impact of silica nanoparticles on the phase transition behavior of phospholipid membranes in theory and experiment

C. Westerhausen[†], F. Strobl[†], R. Herrmann[‡], A. T. Bauer[§], S. W. Schneider[§], A. Reller[‡], A. Wixforth[†], M. F. Schneider[¶*]

* = correspondence author: matschnei@googlemail.com

[†]Experimental Physics I, Institute of Physics and Augsburg Center for Innovative Technologies (ACIT), University of Augsburg, Augsburg, Germany. [‡]Resources strategy, Physics Institute, University of Augsburg, Augsburg, Germany. [§]Department of Dermatology, University Medical Center Mannheim, University of Heidelberg, Mannheim, Germany. [¶]Biological Physics Group, Department of Mechanical Engineering, Boston University, Boston, USA.

abstract:

For the understanding of the interaction of nanoparticles (NPs) and living cells the interaction of NPs with lipid membranes is an integral step. During particle uptake, the membrane has to bend. The fact that, due to the nature of their phase diagram, the modulus of compression of these membranes can vary by more than one order of magnitude requires that both thermodynamic and mechanical aspects of the membrane have to be considered simultaneously. We demonstrate that silica NPs have at least two independent effects on the phase transition of phospholipid membranes: a chemical effect resulting from the finite instability of the NPs in water and secondly a mechanical effect which origins from a bending of the lipid membrane around the NPs.

We report on our recent experiments which allow to clearly distinguish between both effects and present a thermodynamic model including the elastic energy of the membranes, which correctly predicts our findings both quantitatively and qualitatively.

Keywords: DSC, phase transition, supported lipid membranes, encapsulation, silicic acid

I. Introduction

The increasing amount and variety of artificially produced nanometer scale particles calls for a thorough understanding of the influence of such nanoparticles on biological material. Especially the uptake in human cells and its consequences are in the focus of many research teams (1, 2). Silica nanoparticles (NPs) not only occur in exhaust emissions, but are also additives to food, textiles and construction materials to improve their properties (3). Moreover, they are even considered for drug delivery (4). In particular the uptake of NPs by living cells has recently become subject of risk assessments, as it correlates with cytotoxicity (5). In this context, it has been shown before that clathrin-dependent endocytosis is the most important pathway for the cellular uptake of silica-nanoparticles (6). For the detailed understanding of endocytotic mechanisms it is helpful to first study the mechanical properties of pure lipid membranes, which have been shown to be suitable model systems for cell membranes (7). Here, one has to bear in mind that the elastic properties of the lipid membrane depend on its thermodynamic state and can vary substantially. Especially during the transition from the gel to the fluid phase, the bending modulus changes by at least one order of magnitude (8, 9).
Indeed, it has been demonstrated that this phase transition can trigger a variety of morphological transitions even in the absence of membrane proteins. Tube formation, fission, budding as well as the expulsion of entire vesicles have been reported (10-13). The thermodynamic state of the membrane must therefore be definitely considered as an important factor for the understanding of transport mechanisms in cells. The lipid phase transition can be conveniently monitored by Differential Scanning Calorimetry (DSC) which allows to detect even minor changes in the membrane properties (14). In 1992, Naumann et al. were able to demonstrate that 1,2-dipalmitoyl-*sn*-glycero-3-phosphocholine (DPPC) bilayers on a spherical particle support ($R \approx 300$nm) melt cooperatively, but exhibit a suppressed pre-transition (15). Using particles of two different sizes ($R \approx 30$nm, $R \approx 300$nm), it has further been shown that the transition temperature of supported membranes is related to their curvature, i.e. the radius of the particles (16). Finally, for vesicles with diameters below 100nm (17), the same concept has been applied to analyze the influence of differences in the curvatures of the inner and outer leaflet on the melting transition temperature T_m.

Here, we employ DSC to characterize the impact of the same NPs that have been shown to be cytotoxic for human endothelial cells (5) on different phospholipid membranes. We investigate spherical supported vesicles (SSV) in terms of their transition temperature and find significantly different dependencies on the membrane curvature for different lipid-chain-lengths. A thermo-mechanical model is developed being able to explain our experimental findings by including the bending energy of the bilayer into the thermodynamic potential. In addition, a chemically induced depression of T_m is reported, which is triggered by the release of small amounts of silicic acid (SA) from the NPs.

II. Materials and Methods

Silica particles with the following diameters were used: d = 16±2 nm, 18±2 nm, 85±4 nm, 212±25 nm, 305±35 nm and 348±40 nm. All NPs used were synthesized and analyzed as described earlier in detail by Blechinger et al. (6). 1,2-Ditridecanoyl-*sn*-glycero-3-phosphocholine (13:0PC), 1,2-dimyristoyl-*sn*-glycero-3-phosphocholine (DMPC or 14:0PC), 1,2-dipentadecanoyl-*sn*-glycero-3-phosphocholine (15:0PC), 1,2-dipalmitoyl-*sn*-glycero-3-phosphocholine (DPPC or 16:0PC) and 1,2-diarachidoyl-*sn*-glycero-3-phosphocholine (20:0PC), dissolved in chloroform, were obtained from Avanti polar lipids (USA) and used without further purification.
Suspensions of vesicles and NPs were prepared by re-hydrating the dried lipid film with a dispersion of NPs in ultrapure water (pure Aqua, Germany;18,2MΩcm). The final lipid

concentration was 1 mg/ml. For the multi lamellar vesicle (MLV) preparation, the sample was heated above the main phase transition temperature T_m for 60 minutes and vortexed several times. Afterwards, the solution was either sonicated above T_m for 30 min or directly loaded into the calorimeter. The pure NP dispersions as well as the SSV containing sonicated samples were analysed regarding their colloidal stability. Dynamical light scattering analysis shows that the hydrodynamic radius of such samples does not change significantly over typical experimental timescales, i.e. several hours. Also the observation of different dried samples by SEM shows no signs of big agglomerates.
The measurements were carried out with a Microcal VPDSC Differential Scanning Calorimeter (18) at a scan rate of 17 K/h. The reference sample was ultrapure water. The supernatant of centrifuged NP dispersions was analyzed with electrospray ionisation mass spectrometry (ESI-MS, Thermo Finnigan LTQ FT, resolution 100.000 at m/z=400, up to 2000u, 4kV, heating capillary temperature 250°C) to quantify the most frequent oligomers of silicic acid released from the NPs.

III. Results and Discussion

Chemical impact of silica NPs on T_m

When adding NPs to a suspension of MLV, both the main transition and the pre-transition peaks shift towards lower temperatures (see Figure 1A). To quantify this effect, the peak position of the main transition (T_m) was analyzed as a function of particle concentration and size (figure 1B). The mass concentration c_m was chosen such to keep the total *NP surface area per sample* in the same range for all NP sizes. Thus, c_m covers a wider range for the larger NPs (figure 1B). Our experiments revealed the following trend: independent from particle size, the temperature shift of the main transition exhibits a *linear dependence on the total amount of added NP mass* which indicates an effect that is *not* related to the total particle surface. The measurements where then repeated substituting the particles by the supernatants of the centrifuged NP dispersions of adequate particle concentration (10000g, 3min-300min, depending on NP size). Figure 1B shows that the temperature shift of such NP free samples is equal to the corresponding NP containing samples. Therefore, the shift in T_m with increasing concentration *does not* arise from the physical presence of the NPs, but can rather be caused by substances dissolved from the NPs. This is confirmed by the fact that an increase in incubation time of washed NPs, leads to an increasing shift in T_m as well. Alexander et. al. (19) already reported that silica always partially dissolves in aqueous solutions, forming silicic acid oligomers (SA). Using equation 42 of (20) for the used NPs, 95% of the equilibrium concentration of silica in water is reached within nine hours, leading to a concentration of SA in the range of 150 ppm (19, 21). ESI mass spectra showed both tetramers (m/z = 274.8809) and pentamers (m/z = 370.8693) are the most frequent oligomers in our NP dispersions (data not shown).

To confirm that SA is indeed the origin of the decrease in T_m, freshly prepared and oversaturated SA solution was added to MLV samples. A linear decrease in T_m as presented in figure 2 was found.

Regarding the hydrophilic character of SA (22) we expect head group effects to cause the observed melting point depression. One possible explanation could be an altered solvation of both lipid phases in a SA solution compared to water.
Disregarding the specific nature of the SA – lipid interaction, we assume that the soluted SA influences the chemical potentials of gel phase μ_{gel} and fluid phase μ_{fluid}:

$$\mu_i(T) = \mu_i^w(T) + \Delta\mu_i^{tr}(T) \qquad (1)$$

μ_i^w denotes the standart chemical potential of the corresponding lipid phase in water and μ_i^{tr} the free energy associated with a transfer of the phase from water to the solution.
It was shown earlier (23) that for the shift of the transition temperature ΔT_m holds:

$$\Delta T_m = \left[-\frac{RT_m^2}{\Delta H(T_m)}\right] \alpha c_{SA} =: A c_{SA} \qquad (2)$$

where R is the gas constant, T_m the melting temperature of the lipid in pure water, $\Delta H(T_m)$ the change of the systems enthalpy at T_m and c_{SA} the concentration of the solute SA. For low concentrations c_{SA} and small temperature changes, α is a constant that depends on the strength of the interaction of the solute with both phases, i.e. the values of $\mu_{gel}^{tr}(T_m)$ and $\mu_{fluid}^{tr}(T_m)$.
It is noteworthy that the linear dependence of ΔT_m on c_{SA} is true for a direct associative reaction between lipid phases and solute as well as for indirect influences as solvation effects, for instance. Our measurements with oversaturated SA (see fig. 2) suggest a proportionality constant of A= 0,119 mK/ppm.
A very interesting result is that the equilibrium concentration of (SA) in water seems to depend on the amount of dispersed nanoparticles, a phenomenon that cannot be explained when the particles are simply considered as small bulk material but a further examination of that point would be out of the scope of this work.
Here we want to emphasize that silica nanoparticles release amounts of SA which can significantly influence the thermodynamic properties of lipid membranes. The concentration of dissolved SA seems to be approximately proportional to the mass concentration of nano particles in the dispersion, and does not dependent on their size. Future studies should take that effect into account, regardless of the curvature-induced effect explained in the following section.

Development of spherical solid-supported phospholipid bilayers

Storing the samples for one week after preparation led to the occurrence of an additional peak in the DSC profile at a temperature T_s (see Fig.3). After sonication, this additional peak becomes more pronounced than the original one at T_m, indicating an increasing portion of the lipids undergoing the transition at T_s following this step. Furthermore, the samples were centrifuged after sonication at 10000g for 15 to 60 minutes. Before repeating the centrifugation step, the supernatant was replaced with ultrapure water. In the inset of figure 3, the ratio of the transition enthalpies of the additional (ΔH_s) and the main transition (ΔH) are shown before and after centrifugation. While this ratio is only about 0.01 for the untreated sample, it increased to 1 after the first and to 2.2 after the second centrifugation step. This clearly indicates that the additional peak at T_s has its origin in lipids which are attached to the NPs.
This observation and conclusion is consistent with the findings of Naumann et al. and Bayerl et al. (15, 24) who coated NPs with lipid membranes and reported comparable shifts in T_m. Furthermore, in 1996, Brumm et al. showed some differences in the curvature dependence between 14:0PC and 18:0PC, but these reports left the question about a systematical study of the influence of the NP size open.
Hence, the heat capacity profile of the supported membrane population was analyzed both for NPs of different diameters (20 nm - 348 nm) and lipids with different chain lengths between 13 and 20 carbon atoms but identical head group. To account for the above mentioned chemical melting point depression, we analyzed the difference $\Delta T := T_m - T_s$ (see figure 4A) between the transition temperatures of free and supported lipids. Assuming that the above *chemical* effect is of the same order for both experiments, it should cancel out.
All measurements show the same tendency, namely a shift of T_m towards lower temperatures for the solid-supported case. Exemplarily, for 20:0PC the heat capacity profiles are shown in figure 4A for different NP sizes. The expected broadening of the SSV due to decreasing cooperativity with increasing membrane curvature was observed but not analyzed further.

Figure 4B shows ΔT for different lipids and NP diameters. While ΔT decreases with decreasing NP diameter for 13:0PC, 14:0PC and 15:0PC, it increases for 16:0PC and 20:0PC. For all lipids, except for 20:0PC, the limit for a "flat" support of zero curvature is roughly ΔT = 2,5 K.
To summarize, our results consist of three main observations: i) for all lipids and NP sizes, T_s shifts towards lower temperatures, with a ΔT ranging between 0.5 K and 4 K, ii) the curvature dependence changes its sign for increasing chain length and iii) for all lipids, ΔT shows a saturation behavior with decreasing curvature.

Theory. Bending contribution to ΔT

In the case of SSV, the vesicles spread on and cover the NPs or parts of them, hence experiencing a curved substrate. In the following paragraph, an analytical expression for the expected change in phase transition temperature T_m based on the mechanical and calorimetric properties of the system will be derived. We therefore integrate the bending energy of the membrane in a Landau-type potential. No new or additional model assumptions are introduced. Instead, we combine existing theories to provide a coherent explanation of our results.

Contributions to the Landau potential

In the Landau theory, a first order phase transition is represented by the relative evolution of the double well potential of the form shown in figure 5 (25, 26):

$$\Phi(P,T,\Pi,\eta) = \Phi_0 + A\eta^2 + B\eta^4 + C\eta^6 \qquad (3)$$

Here, η is the order parameter and $A(T,p,\Pi)$, $B(p,\Pi)$, $C(p,\Pi)$ are functions of the thermodynamic variables temperature T, bulk pressure p and lateral pressure Π.

It is convenient and common to consider only the evolution of the potential minima in η with temperature. These are then identified with the Gibbs Free Energy potentials for the gel phase and the fluid phase (27, 28) as indicated in figure 6.

In the absence of any solid support, the two potentials intersect at the phase transition temperature T_m. The additional energies $\Delta G_{gel}$and ΔG_{fluid} (see Fig. 5) in the presence of the support shifts the intersection towards lower temperatures T_s. For the transition temperature T_s now holds:

$$G_{gel}(T_S) + \Delta G_{gel} = G_{fluid}(T_S) + \Delta G_{fluid} \qquad (4)$$

Assuming p to be constant and $\frac{\partial^2 \pi}{\partial T^2} \approx 0$ as shown in (29), $G_{gel}(T)$ and $G_{fluid}(T)$ can be approximated by a first order Taylor series near the transition point T_m:

$$G_{gel}(T_m) + \frac{\partial G_{gel}}{\partial T}\Big|_{T_M} (T_S - T_m) + \Delta G_{gel} = G_{gel}(T_m) + \frac{\partial G_{fluid}}{\partial T}\Big|_{T_M} (T_S - T_m) + \Delta G_{fluid} \qquad (5)$$

and consequently:

$$\Delta T := T_m - T_S = \frac{\Delta G_{gel} - \Delta G_{fluid}}{\left(\frac{\partial G_{gel}}{\partial T}\Big|_{T_M} - \frac{\partial G_{fluid}}{\partial T}\Big|_{T_M}\right)} =: \frac{\Delta G_{gel} - \Delta G_{fluid}}{\Delta\left(\frac{\partial G}{\partial T}\right)} \qquad (6)$$

This general *analytical* expression connects the contribution of the solid support to the free energy $\Delta G_{gel/fluid}$ with the shift of the transition temperature ΔT.

$\Delta \frac{\partial G}{\partial T}$ *from the heat capacity profile*

$\Delta \frac{\partial G}{\partial T}$ can be extracted from the experimental DSC data, recalling the relation between the thermodynamic potential G and the heat capacity c_p as its susceptibility:

$$-T\frac{\partial^2 G}{\partial T^2}|_p = T\frac{\partial S}{\partial T}|_p = c_p \qquad (7)$$

In agreement with the linear approximation that was described above, we have to integrate over $\frac{\partial^2 G}{\partial T^2}$ (respectively c_p) in the transition region to get $\Delta \frac{\boldsymbol{\partial G}}{\boldsymbol{\partial T}}$:

$$\Delta\frac{\boldsymbol{\partial G}}{\boldsymbol{\partial T}} = \int_{\boldsymbol{T_1}}^{\boldsymbol{T_2}} \frac{\partial^2 G}{\partial T^2} dT = -\int_{\boldsymbol{T_1}}^{\boldsymbol{T_2}} \frac{\boldsymbol{c_p}}{\boldsymbol{T}} \mathrm{dT} \approx -\frac{\Delta \mathrm{H}}{T_m} \qquad (8)$$

The last approximation introduces the transition enthalpy ΔH and holds for sharp transitions for which a constant temperature T_m can safely be assumed.

Mechanical contributions to ΔG

In the case of SSV, we consider two main contributions to ΔG: i) a curvature dependent one caused by the bending of the membrane and ii) a curvature independent one due to the bare presence of the substrate (planar limit). The latter, constant contribution to ΔG can be caused by various interactions between lipids and support, for example by electrostatic forces.
To describe the mechanical contribution due to curvature, we use the well-known (30) expression for the bending energy E_{bend} of a membrane. For the curvature independent contribution we add an additional constant contribution G_s:

$$\Delta \mathrm{G} = E_{bend} + G_s \approx \frac{1}{2}\left(\frac{2}{R} - \frac{1}{R_0}\right)^2 \kappa A_{mem} + \frac{1}{R^2}\kappa_G A_{mem} + G_s \qquad (9).$$

Here, A_{mem} is the area of the lipid bilayer, $\frac{1}{R_0}$ is the spontaneous curvature, κ the bending modulus and κ_G the modulus of Gaussian curvature. In the case of a chemically symmetric bilayer, the spontaneous curvature is caused by the asymmetry of the environment due to the NP and a thin layer of water inside and the bulk water outside the vesicle. The bending radius R is simply determined by the radius R of the particle.

Due to the higher flexibility of lipid membranes in the fluid phase, we assume a stronger contribution of the mechanical bending energy to Φ for the low symmetric gel phase (fig. 5.). Therefor we neglect the bending energy contribution to ΔG_{fluid} and hence the final expression for the temperature shift ΔT can then be found by combining eq. 6, eq. 8 and eq. 9:

$$\Delta T = T_m \frac{\frac{1}{2}\left(\frac{2}{R}-\frac{1}{R_0}\right)^2 \kappa A_{mem}+\frac{1}{R^2}\kappa_G A_{mem}+ G_{Sgel}- G_{Sfluid}}{\Delta H} \stackrel{\text{def}}{=} =$$

$$T_m \frac{\frac{1}{2}\left(\frac{2}{R}-\frac{1}{R_0}\right)^2 \kappa A_{mem}+\frac{1}{R^2}\kappa_G A_{mem}+ \Delta G_S}{\Delta H} \qquad (10)$$

This expression explicitly relates the shift ΔT of the main phase transition temperature with the mechanical and the calorimetric properties of the membrane and predicts trends which can be compared to the experiments.

Discussion – Bending energy explains the curvature dependence of ΔT

In figure 7, we show that our thermodynamic model can indeed well explain the observed trends of the temperature shift for different chain lengths. Eq. 10 was fitted to the data points of fig. 4B. Here T_m and ΔH were taken from the heat capacity profiles, κ was set to 2,5 10^{-18}J for 16:0PC and estimated according to κ = 2,5 10^{-18}J$(h/16)^3$ for the other lipids (31, 32) where, h is the number of carbon atoms of the hydrophobic chains of the lipids. Furthermore A_{mem} was set as 0,5nm² and R is the radius of the NPs. Thus there are three unknown parameters ΔG_s, κ_G and $\frac{1}{R_0}$. As the head groups of all lipids are the same it is reasonable to consider ΔG_s as constant. For this reason we initially perform a three parameter fit to get an idea about the magnitude of ΔG_s (see SM fig. 3a). Then ΔG_s was set to a fixed value ΔG_s=150J/mol resulting in a two parameter fit (fig. 7). Figure 7 shows an excellent qualitative and satisfying quantitative agreement between the analytical expression (eq. 10) and the experiments:

The order of magnitude, the range, the inversion of the curvature dependence and the quantitative shifts are predicted correctly. In the following the results for the parameters $z := \frac{\kappa_G}{\kappa}$ and $c_0 := \frac{1}{R_0}$ are discussed.

The fit results in values of z ≈ -2 (for details see SM fig. 2) in accordance with theoretical predictions (33, 34). In (33) it is shown that you can calculate κ_G as the second moment of the stress profile of the bilayer cross section. Using a simplified stress profile we show in the supplementary material that for lipids with the same head group κ_G results as a quadratic function of the chain length h, what is in good accordance with our values from the fit (see SM Fig.4). As also simulations of simple amphiphilic molecules show a similar dependence of the bending moduli as function of the chain length, the results seem convincing.

On the other hand the resulting values for the spontaneous curvature are more curious. As shown in SM fig. 2 for almost lipids we get negative c_0 ≈ -0,005. For the exception 13:0PC the spontaneous curvature is almost negligible. Intuitively we would expect a decrease in spontaneous curvature with increasing membrane thickness. This is still an open question that we cannot explain yet. But at least as the origin of the asymmetry in our case lies in the environment and not in the membrane composition, it is not surprising that we extract smaller values than those reported earlier (35).

Further sources of error can be the omitting of the bending energy contribution of the fluid phase to ΔG and the assumption of a constant A_{mem} for all lipids. But the aim of this work was not the precise determination of the exact values of the spontaneous curvature of this particular case of silica NP and those lipids. We looked for a coherent model that predicts the right order of magnitude of ΔT and the occurring trends with increasing curvature. For sure we can reason that z ≈ -2, as otherwise the resulting bending energy contributions would already predict for relative small NP curvatures much too big shifts in melting temperature.

IV Conclusion

In summary, we present in-depth theoretical and experimental studies on nano particle – membrane interaction showing that silica NPs are able to influence the thermodynamic state of lipid membranes via at least two different mechanisms. First, a melting point depression caused by silicic acid released from the NPs in aqueous solution has been clearly identified. This finding calls for a thorough analysis of the chemical stability of NPs before studying their interaction with biological matter, because even minute amounts of membrane-soluble substances can change the thermodynamic properties of the membranes significantly. Apart from this rather chemical aspect, we also find indeed a size dependent impact of silica nanoparticles on the thermodynamic properties of phospholipid membranes mediated by the bending energy of the membrane. An analytical expression to describe the shift in T_s of solid-supported lipid bilayers by thermodynamic and mechanical considerations was proposed. Together with further experimental data this could offer a way to estimate the modulus of Gaussian curvature of lipid membranes, a parameter that is very difficult to access otherwise.
Finally, we like to point out that earlier work has demonstrated, that ion permeability, morphological changes or adhesion phenomena can be controlled by a shift in the thermodynamic state of the lipid membranes (11, 12, 27, 36). A comparison between these data and the shift in state by NPs observed here, demonstrates that NPs are in principle capable to induce the phenomena mentioned. We believe that these induced changes in membrane state are of biological relevance and it will be highly interesting to test this hypothesis systematically in experiments similar like those reported in Bauer et. al.(5), where we showed with identical NPs that the decrease in viability of cells was direct proportional to the total provided NP surface area. From our results we expect a shift in membrane order upon contact with the NP and correlation between the change in membrane phase transition and cytotoxicity.

Acknowledgement:
We thank our cooperating group of Prof. C. Bräuchle, Ludwig-Maximilians-Universität, Munich for the mass spectroscopy measurements. This work was financially supported by the Nanosystems Initiative Munich and by the DFG through the SPP1313 BIOMEM (A. Reller, M. F. Schneider, S. Schneider, A. Wixforth).

References

1. Greulich, C., S. Kittler, M. Epple, G. Muhr, and M. Köller. 2009. Studies on the biocompatibility and the interaction of silver nanoparticles with human mesenchymal stem cells (hMSCs). Langenbeck's Archives of Surgery 394:495–502.
2. Rothen-Rutishauser, B., R. N. Grass, F. Blank, L. K. Limbach, C. Mühlfeld, C. Brandenberger, D. O. Raemy, P. Gehr, and W. J. Stark. 2009. Direct Combination of Nanoparticle Fabrication and Exposure to Lung Cell Cultures in a Closed Setup as a Method To Simulate Accidental Nanoparticle Exposure of Humans. Environmental Science & Technology 43:2634–2640.
3. Knauer S., S. R. 2009. controversy at the „Nanohype“: Nanoparticel – friend or enemy? DZKF 5-6:20–26.
4. Barbé, C., J. Bartlett, L. Kong, K. Finnie, H. Q. Lin, M. Larkin, S. Calleja, A. Bush, and G. Calleja. 2004. Silica Particles: A Novel Drug-Delivery System. Advanced Materials 16:1959-1966.
5. Bauer, A. T., E. Strozyk, C. Gorzelanny, C. Westerhausen, A. Desch, M. F. Schneider, and S. W. Schneider. 2011. Surface area-dependent Cytotoxicity of Silica Nanoparticles induces Exocytosis of von Willebrand factor and necrotic Cell Death in primary human endothelial Cells.
6. Blechinger, J., R. Herrmann, D. Kiener, F. J. García-García, C. Scheu, A. Reller, and C. Bräuchle. 2010. Perylene-Labeled Silica Nanoparticles: Synthesis and Characterization of Three Novel Silica Nanoparticle Species for Live-Cell Imaging. Small 6:2427–2435.

7. Simons, K., and W. L. C. Vaz. 2004. MODEL SYSTEMS, LIPID RAFTS, AND CELL MEMBRANES 1. Annual Review of Biophysics and Biomolecular Structure 33:269–295.
8. Heimburg, T. 2007. Thermal Biophysics of Membranes. Wiley-VCH Verlag GmbH & Co. KGaA.
9. Kwok, R., and E. Evans. 1981. Thermoelasticity of large lecithin bilayer vesicles. Biophysical Journal 35:637–652.
10. Roux, A., D. Cuvelier, P. Nassoy, J. Prost, P. Bassereau, and B. Goud. 2005. Role of curvature and phase transition in lipid sorting and fission of membrane tubules. The EMBO Journal 24:1537–1545.
11. Leirer, C., B. Wunderlich, V. M. Myles, and M. F. Schneider. 2009. Phase transition induced fission in lipid vesicles. Biophysical Chemistry 143:106–109.
12. Franke, T., C. T. Leirer, A. Wixforth, N. Dan, and M. F. Schneider. 2009. Phase-Transition- and Dissipation-Driven Budding in Lipid Vesicles. ChemPhysChem 10:2852–2857.
13. Leirer, C. T., and et al. 2009. Thermodynamic relaxation drives expulsion in giant unilamellar vesicles. Physical Biology 6:016011.
14. Seelig, J. 2004. Thermodynamics of lipid-peptide interactions. Biochimica et Biophysica Acta (BBA) - Biomembranes 1666:40–50.
15. Naumann, C., T. Brumm, and T. M. Bayerl. 1992. Phase transition behavior of single phosphatidylcholine bilayers on a solid spherical support studied by DSC, NMR and FT-IR. Biophysical Journal 63:1314–1319.
16. Brumm, T., K. Jørgensen, O. G. Mouritsen, and T. M. Bayerl. 1996. The effect of increasing membrane curvature on the phase transition and mixing behavior of a dimyristoyl-sn-glycero-3-phosphatidylcholine/ distearoyl-sn-glycero-3-phosphatidylcholine lipid mixture as studied by Fourier transform infrared spectroscopy and differential scanning calorimetry. Biophysical Journal 70:1373–1379.
17. Ahmed, S., and S. L. Wunder. 2009. Effect of High Surface Curvature on the Main Phase Transition of Supported Phospholipid Bilayers on SiO 2 Nanoparticles. Langmuir 25:3682–3691.
18. Plotnikov, V. V., J. M. Brandts, L.-N. Lin, and J. F. Brandts. 1997. A New Ultrasensitive Scanning Calorimeter. Analytical Biochemistry 250:237–244.
19. Alexander, G. B., W. M. Heston, and R. K. Iler. 1954. The Solubility of Amorphous Silica in Water. Journal of Physical Chemistry 58:453–455.
20. Rimstidt, J. D., and H. L. Barnes. 1980. The kinetics of silica-water reactions. Geochimica et Cosmochimica Acta 44:1683–1699.
21. O'Connor, T. L., and S. A. Greenberg. 1958. The kinetics for the solution of silica in aqueous solutions. Journal of Physical Chemistry 62:1195–1198.
22. Iler, R. K. 1979. The chemistry of silica. John Wiley & Sons.
23. Chapman, D., W. E. Peel, B. Kingston, and T. H. Lilley. 1977. Lipid phase transitions in model biomembranes. The effect of ions on phosphatidylcholine bilayers. Biochim Biophys Acta 464:260-275.
24. Bayerl, T. M., and M. Bloom. 1990. Physical properties of single phospholipid bilayers adsorbed to micro glass beads. A new vesicular model system studied by 2H-nuclear magnetic resonance. Biophysical Journal 58:357–362.
25. Landau, L. D. 1987. Statistische Physik. Akad.-Verl., Berlin.
26. Callen, H. 1985. Thermodynamics and an Introduction to Thermostatistics, 2nd Edition. Wiley-VCH.
27. Schneider, M. F. 1999. Network formation of lipid membranes: Triggering structural transitions by chain melting. Proceedings of the National Academy of Sciences 96:14312–14317.
28. Träuble, H., M. Teubner, P. Woolley, and H. Eibl. 1976. Electrostatic interactions at charged lipid membranes: I. Effects of ph and univalent cations on membrane structure. Biophysical Chemistry 4:319–342.

29. Steppich, D., J. Griesbauer, T. Frommelt, W. Appelt, A. Wixforth, and M. Schneider. 2010. Thermomechanic-electrical coupling in phospholipid monolayers near the critical point. Physical Review E 81.
30. Helfrich, W. 1973. Elastic properties of lipid bilayers: theory and possible experiments. Z. Naturforsch:pp. 693-703.
31. Seto, H., N. L. Yamada, M. Nagao, M. Hishida, and T. Takeda. 2008. Bending modulus of lipid bilayers in a liquid-crystalline phase including an anomalous swelling regime estimated by neutron spin echo experiments. The European Physical Journal E 26:217–223.
32. Marsh, D. Elastic curvature constants of lipid monolayers and bilayers. Chemistry and Physics of Lipids 144:146–159.
33. Helfrich, W. 1981. Physics of defects, Amsterdam and New York.
34. Helfrich, W. 1994. Lyotropic lamellar phases. Journal of Physics: Condensed Matter 6:A79.
35. Zimmerberg, J., and M. M. Kozlov. 2005. How proteins produce cellular membrane curvature. Nature Reviews Molecular Cell Biology 7:9–19.
36. Wunderlich, B., C. Leirer, A.-L. Idzko, U. F. Keyser, A. Wixforth, V. M. Myles, T. Heimburg, and M. F. Schneider. 2009. Phase-State Dependent Current Fluctuations in Pure Lipid Membranes. Biophysical Journal 96:4592–4597.

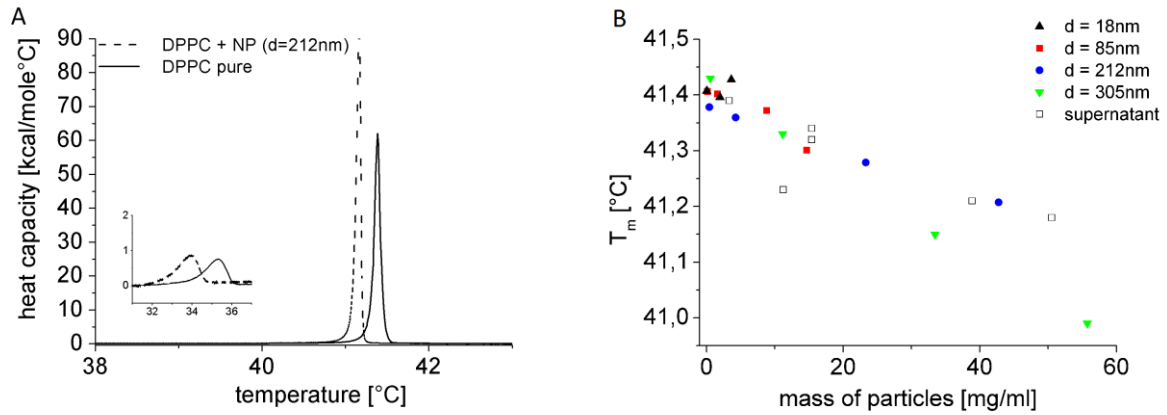

Figure1

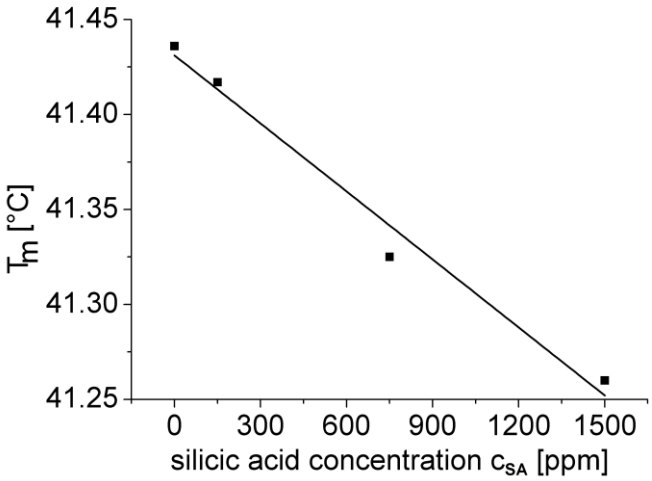

Figure 2

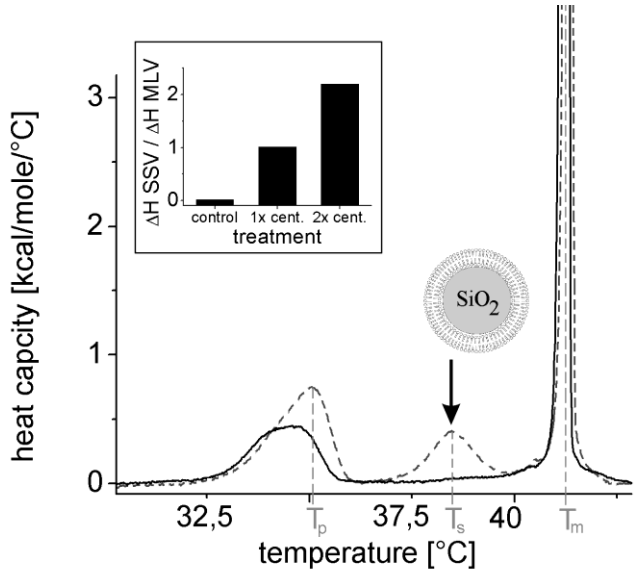

Figure 3

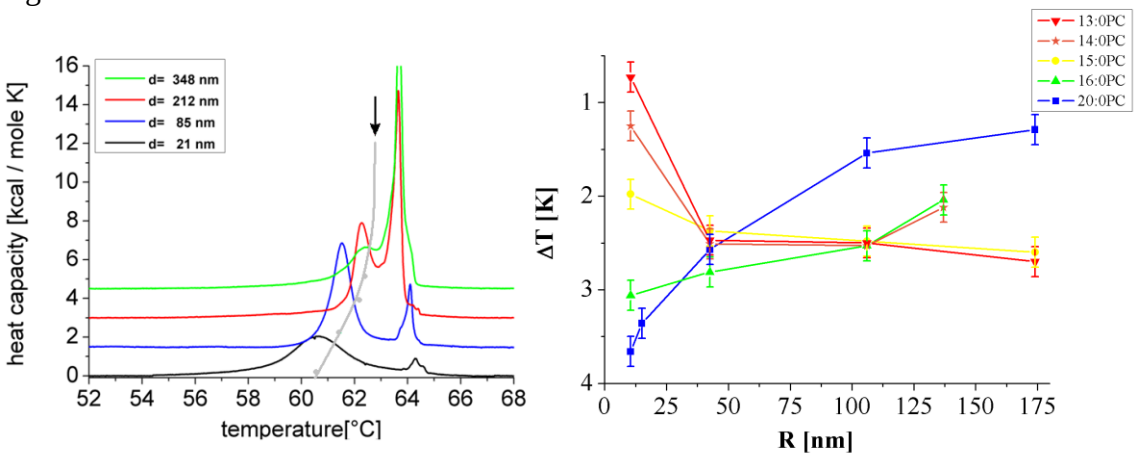

Figure 4

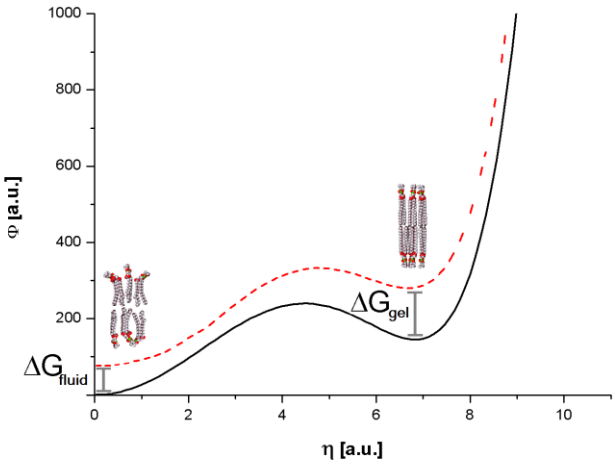

Figure 5

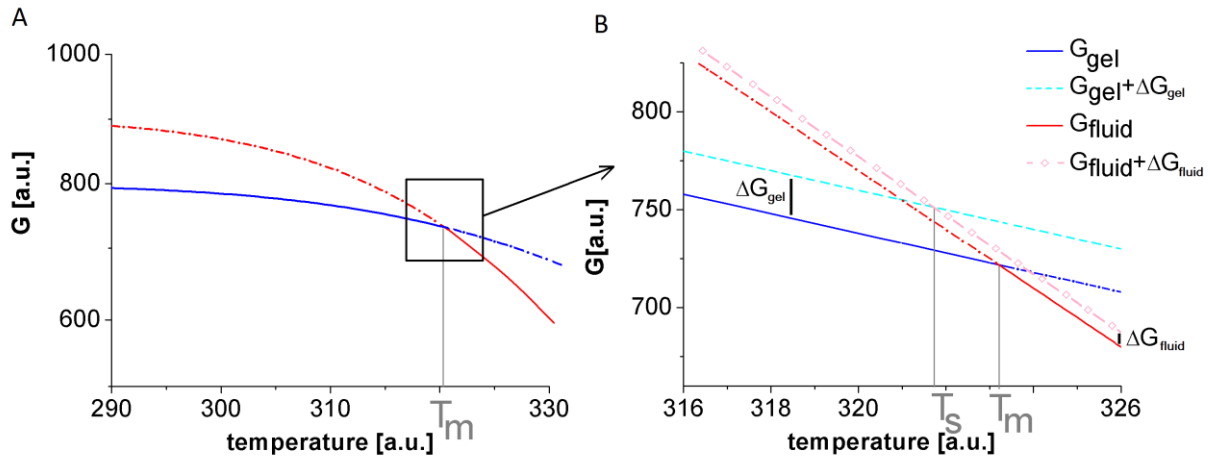

Figure 6

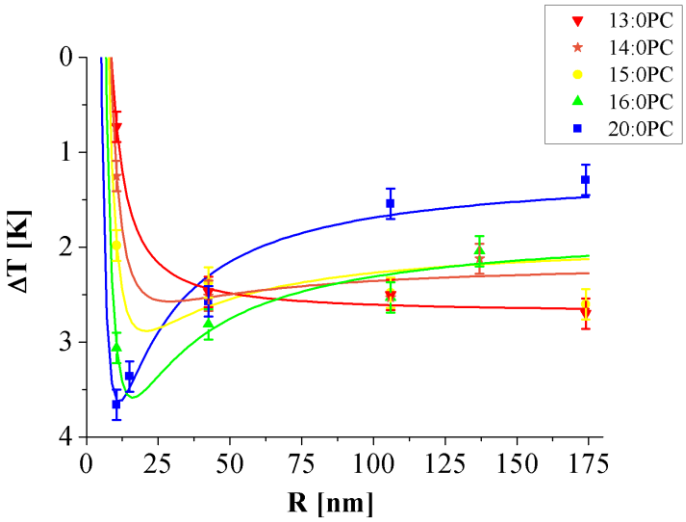

Figure 7